# LOW-ENERGY ELECTRON TRANSPORT WITH THE METHOD OF DISCRETE ORDINATES[1]

D. E. Bartine, R. G. Alsmiller, Jr.,
F. R. Mynatt, W. W. Engle, Jr.,
and J. Barish

Oak Ridge National Laboratory
Oak Ridge, Tennessee, 37830

The one-dimensional discrete ordinates code ANISN has been adapted to transport low-energy (∿ a few MeV) electrons. Calculated results obtained with ANISN are compared with experimental data for the transmitted electron energy and angular distributions for 1-MeV electrons normally incident on aluminum slabs of several thicknesses. The calculated and experimental results to date are in good agreement for a thin slab (0.2 of the electron range) but are not in good agreement for thicker slabs (0.6 of the electron range). Calculated results obtained with ANISN are also compared with calculated results obtained using Monte Carlo methods.

## INTRODUCTION

The transport of low-energy (of the order of a few MeV) electrons through matter is important in the shielding of manned space vehicles that pass through the Van Allen electron belt. A code that treats this transport by means of Monte Carlo methods is available (ref. 1), but because of the poor statistical accuracy which can be obtained in some cases, a nonstatistical method of calculation is needed. To fill this need, the method of discrete ordinates has been adapted to the transport of low-energy electrons. The method of calculation is discussed in the next section, and the calculated results are presented and compared with experimental results and other calculated data in the last section.

## METHOD OF CALCULATION

In principle, the discrete ordinates code ANISN (ref. 2) may be used to transport electrons by the simple expedient of introducing into the code the differential cross sections for electron-nucleus elastic collisions, electron-nucleus bremsstrahlung-producing collisions, and electron-electron collisions. In practice, however, these cross sections are quite different from those which occur in neutron transport where the method of discrete ordinates has been used extensively, and the method has shown only partial success in transporting electrons.

In the Monte Carlo treatment of electron transport, the individual electronic collisions are not considered, but rather the theories of multiple Coulomb scattering and continuous slowing down are used to group together large numbers of collisions (ref. 1). In the work reported here, the individual electronic collisions are treated except that those electron-electron collisions which result in very small energy transfers (of the order of the average ionization potential of the atom) are treated using the continuous slowing-down approximation. The equation solved is the Boltzmann transport equation with a continuous slowing-down term added:

$$\vec{\Omega}\cdot\nabla\phi(\vec{R},E,\vec{\Omega}) = P(\vec{R},E,\vec{\Omega})$$

$$+ n\int_{E}^{E_o} dE' \int d\Omega' \frac{d^2\sigma_{e\to e}(E',E,\vec{\Omega}'\cdot\vec{\Omega})}{dE d\Omega}\,\phi(\vec{R},E',\vec{\Omega}')$$

$$+ \int_{E+I'}^{E_o} \int d\Omega' \frac{d^2\sigma_{in}(E',E,\vec{\Omega}'\cdot\vec{\Omega})}{dE d\Omega}\,(\vec{R},E',\vec{\Omega}')$$

$$- n\,\sigma^T(E)\,\phi(\vec{R},E,\vec{\Omega})$$

$$+ \frac{\partial}{\partial E}\left[S(E)\,\phi(\vec{R},E,\vec{\Omega})\right], \qquad (1)$$

[1]This work was funded by the National Aeronautics and Space Administration, Order H-38280A, under Union Carbide Corporation's contract with the U. S. Atomic Energy Commission.

$$\frac{d^2\sigma_{e\to e}(E',E,\vec{\Omega}'\cdot\vec{\Omega})}{dEd\Omega} = \frac{d^2\sigma_{el}(E',E,\vec{\Omega}'\cdot\vec{\Omega})}{dEd\Omega} + \frac{d^2\sigma_{br}(E',E,\vec{\Omega}'\cdot\vec{\Omega})}{dEd\Omega} ,$$

$$\sigma^T_{e\to e}(E') = \int dE \int d\Omega \frac{d^2\sigma_{e\to e}(E',E,\vec{\Omega}'\cdot\vec{\Omega})}{dEd\Omega} ,$$

$$\sigma^T_{in}(E') = \int dE \int d\Omega \frac{d^2\sigma_{in}(E',E,\vec{\Omega}'\cdot\vec{\Omega})}{dEd\Omega} ,$$

$$\sigma^T(E') = \sigma^T_{e\to e}(E') + \sigma^T_{in}(E') ,$$

where

$\vec{R}$ = a vector denoting the position of the particle;

$\vec{\Omega}$ = a unit vector in the direction of the momentum vector;

$d\Omega$ = an element of solid angle;

$E$ = the kinetic energy of an electron;

$\phi(\vec{R},E,\vec{\Omega})$ = the electron flux per unit energy;

$E_o$ = the highest kinetic energy considered;

$n$ = the atomic number density;

$P(\vec{R},E,\vec{\Omega})$ = the number of electrons per unit energy per steradian per unit volume input at R from an external source;

$\frac{d^2\sigma_{el}(E',E,\vec{\Omega}'\cdot\vec{\Omega})}{dEd\Omega}$ = the differential cross section for an electron (E') going in direction $\vec{\Omega}'$ to undergo elastic nuclear scattering (Coulomb scattering) to $(E,\vec{\Omega})$;

$\frac{d^2\sigma_{br}(E',E,\vec{\Omega}'\cdot\vec{\Omega})}{dEd\Omega}$ = the differential cross section for an electron $(E',\vec{\Omega}')$ to undergo bremsstrahlung (radiative) scattering with both nuclei and atomic electrons to $(E,\vec{\Omega})$;

$\frac{d^2\sigma_{in}(E',E,\vec{\Omega}'\cdot\vec{\Omega})}{dEd\Omega}$ = the differential cross section for an electron $(E',\vec{\Omega}')$ to undergo inelastic scattering from atomic electrons to $(E,\vec{\Omega})$, thereby producing a secondary electron with energy E'-E;

$I'$ = an arbitrary value taken to be the minimum energy loss allowed in an inelastic electron-electron collision;

$S(E)$ = the stopping power (energy loss per unit path length) due to inelastic electron-electron collisions resulting in an energy loss smaller than I' (these collisions are presumed to be straightahead).

The differential cross sections for electron-nucleus elastic collisions and electron-nucleus or electron-electron bremsstrahlung production are taken from standard sources (refs. 3 to 5). The differential cross section given by Moller (refs. 3, 6) is used to describe electron-electron collisions which result in large energy transfers ($\geq I'$). The stopping power used to treat electron-electron collisions resulting in small energy transfers ($< I'$) is obtained in the manner outlined by Rohrlich and Carlson (ref. 7) with the density effect correction taken from Sternheimer (refs. 8, 9). The I' value used in the cases reported here is 0.0163 MeV, i.e., 100 × I where I is the average ionization potential for aluminum, 163 eV (ref. 8).

## RESULTS AND DISCUSSION

Goudsmit and Saunderson have obtained an analytic expression for the angular distribution of transmitted electrons when monoenergetic electrons are normally incident on sufficiently thin slabs so that the energy degradation of the electrons may be neglected (ref. 10). Using the Goudsmit-Saunderson theory, Berger obtained the angular distribution of the transmitted electrons resulting from 1-MeV electrons normally incident on an aluminum slab of thickness 0.0287 g/cm$^2$ (ref. 11). The transmitted angular current of electrons calculated by Berger is represented by the histogram shown in figure 1. Also shown in the figure are the results obtained for this same case with the discrete ordinates code ANISN. In the ANISN calculation, one energy group with a range from 1.0106 MeV to 0.9894 MeV and a midpoint of 1.0 MeV were used. No energy degradation was allowed and only elastic scattering was permitted; i.e., in this calculation equation 1 with $\sigma_{in} = \sigma_{br} = S(E) = 0$ was solved. The two calculations shown in figure 1 are in excellent agreement, and thus the method of discrete ordinates can handle satisfactorily small-angle multiple Coulomb scattering.

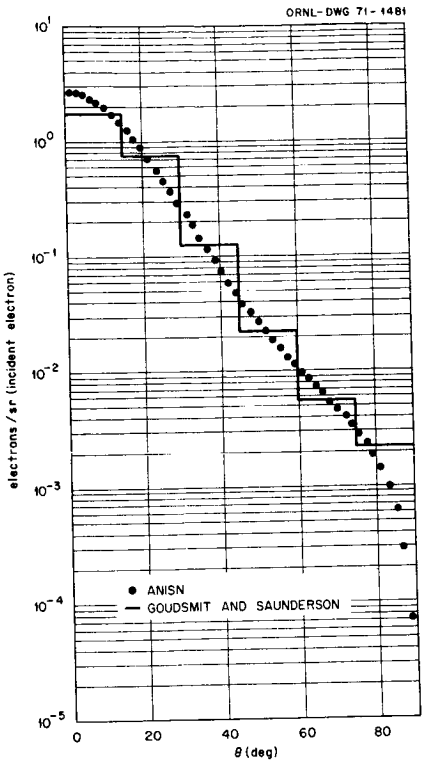


FIGURE 1.— Angular distribution of transmitted electron current for 1-MeV electrons normally incident on a 0.0287-g/cm$^2$-thick aluminum slab.

Rester and Rainwater (ref. 12) and Rester and Dance (ref. 13) have measured the transmitted electron current per unit energy from monoenergetic electrons normally incident on aluminum slabs of varying thicknesses. The solid histograms in figures 2, 3, and 4 show the measured transmitted electron current per unit energy for aluminum slabs of thicknesses of 0.11 g/cm$^2$, 0.22 g/cm$^2$, and 0.33 g/cm$^2$, respectively. Also shown in the figures are calculated results obtained with ANISN (solid curves) and calculated results obtained with the Monte Carlo transport code ETRAN of Berger and Seltzer (ref. 1). In figure 2, the agreement between the ANISN results and the experimental data is very good except at the very highest energies, and in this case, i.e., for a 0.11-g/cm$^2$-thick slab, the ANISN results are in slightly better agreement with the experimental data than the results given by ETRAN. In figure 3, neither ANISN nor ETRAN is in good agreement with the experimental data. In figure 4, which shows results for a relatively thick slab, 0.33 g/cm$^2$ (0.6 of the electron range), the Monte Carlo calculation is in very good agreement with the experimental data, while the ANISN calculation is in very poor agreement. The reason for the progressive failure of the continuous slowing-down ANISN calculation as the thickness increases is not known.

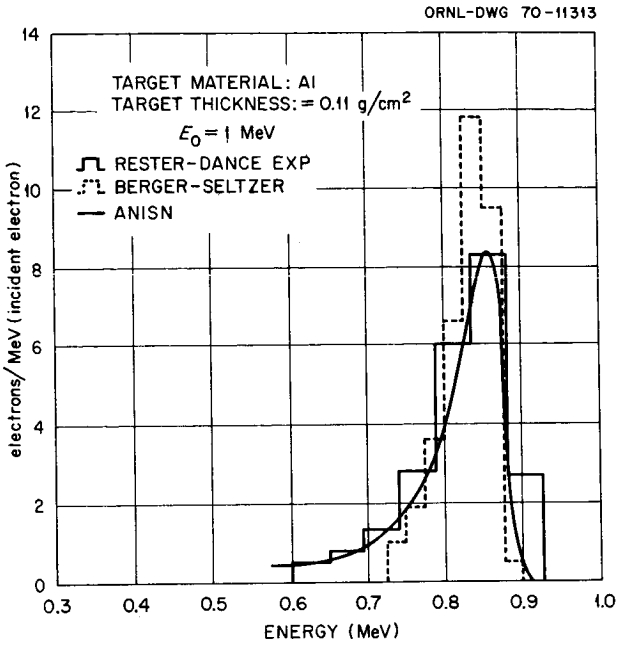


FIGURE 2.— Transmitted electron current per unit energy per incident electron for 1-MeV electrons normally incident on a 0.11-g/cm$^2$-thick aluminum slab.

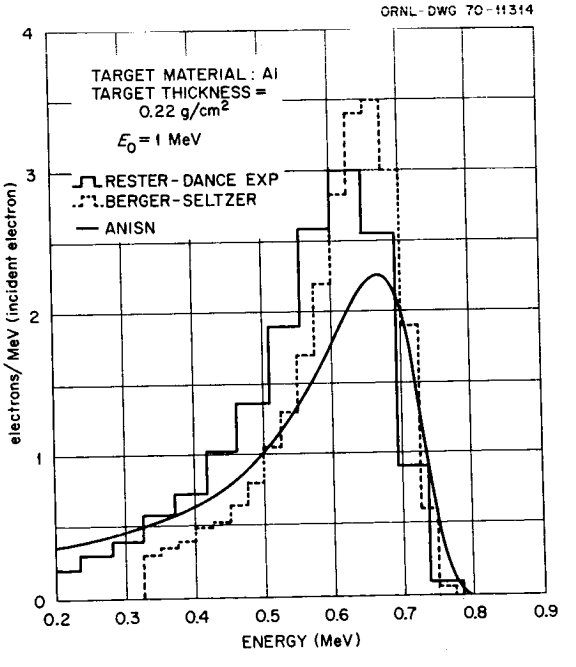


FIGURE 3.— Transmitted electron current per unit energy per incident electron for 1-MeV electrons normally incident on a 0.22-g/cm$^2$-thick aluminum slab.

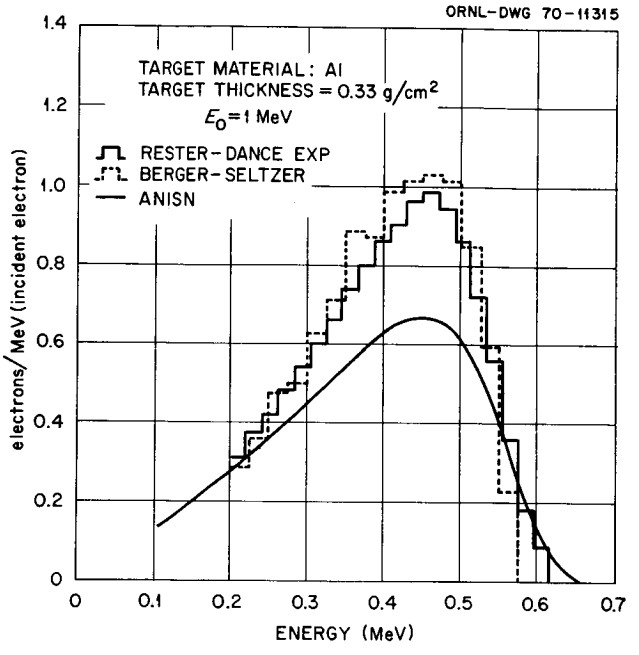


FIGURE 4.— Transmitted electron current per unit energy per incident electron for 1-MeV electrons normally incident on a 0.33-g/cm$^2$-thick aluminum slab.

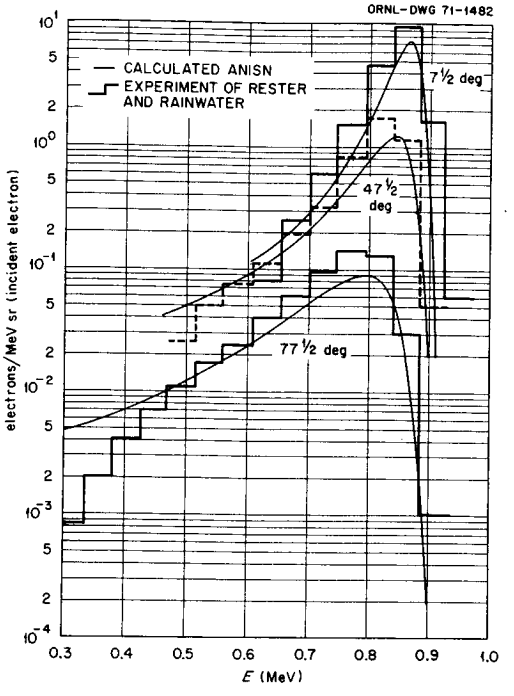


FIGURE 5.— Energy distribution of transmitted electron current at the specific angles indicated for 1-MeV electrons normally incident on a 0.11-g/cm$^2$-thick aluminum slab.

The calculated and measured transmitted electron current per unit energy and per unit solid angle is shown in figure 5 as a function of energy at several angles for a 0.11-g/cm$^2$-thick aluminum slab. The calculated results agree fairly well with the experimental data at all angles, thus indicating an acceptable energy-angle correlation.

Because of the lack of experimental data, it was not possible to present a comparison between calculation and experiment for the case of an electron spectrum incident on a slab. Using the Monte Carlo code ETRAN of Berger and Seltzer (ref. 1), Scott (ref. 14) calculated the transmitted electron current per unit energy for the case of a specific electron energy spectrum normally incident on aluminum slabs, and this theoretical calculation was compared with results obtained with ANISN. The incident electron energy distribution used in the calculations is a representation of the spectrum resulting from thermal neutron capture in $^{235}U$ (ref. 15). This spectrum extends to electron energies of the order of 10 MeV and is shown explicitly in reference 14.

The ETRAN results for an aluminum slab 0.5 g/cm$^2$ thick are shown in figure 6 as a histogram and the ANISN results are shown as plotted points. A similar comparison is given in figure 7 for an aluminum slab 1.0 g/cm$^2$ thick. In both figures 6 and 7 the ETRAN and ANISN results are in very good agreement. Thus, ANISN is apparently capable of treating accurately the transport of low-energy (< 10 MeV) electrons through relatively thick shields in some cases, e.g., the cases considered in figures 6 and 7, but not in all cases, e.g., figures 3 and 4.

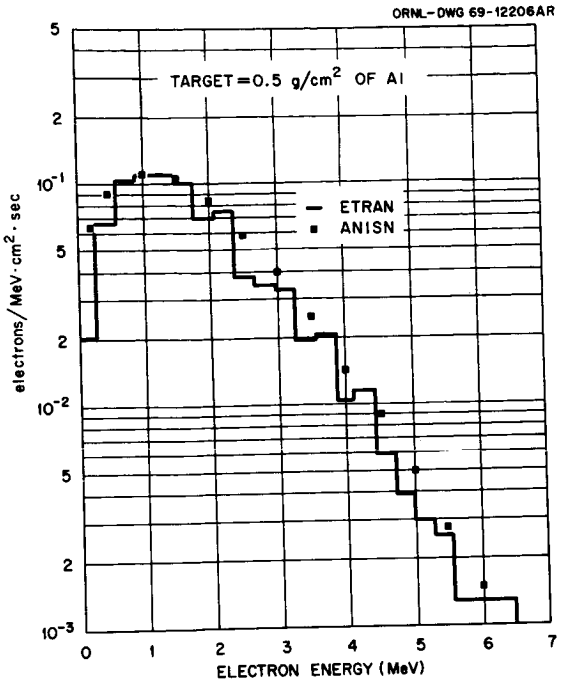


FIGURE 6.— Transmitted electron current per unit energy per incident electron for a specific energy spectrum (ref. 15) normally incident on a 0.5-g/cm$^2$-thick aluminum slab.

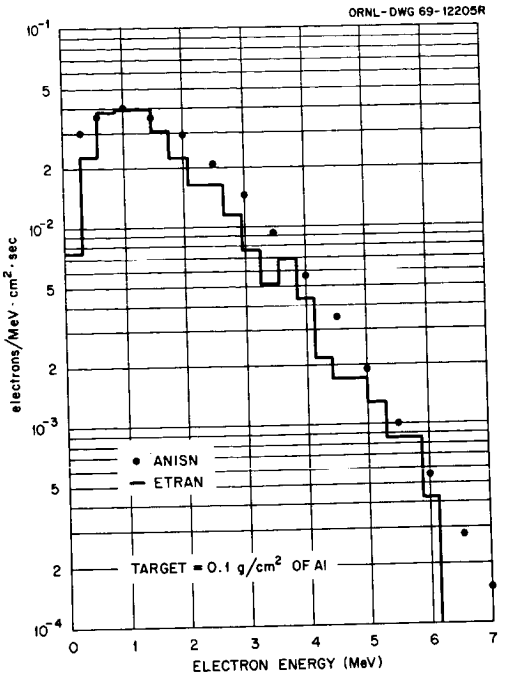


FIGURE 7.— Transmitted electron current per unit energy per incident electron for a specific energy spectrum (ref. 15) normally incident on a 1.0-g/cm$^2$-thick aluminum slab.

## REFERENCES


1. BERGER, M. J.; and SELTZER, S. M.: ETRAN, Monte Carlo Code System for Electron and Photon Transport Through Extended Media, National Bureau of Standards Documents NBS-9836, 1968, and NBS-9837, 1968.
2. ENGLE, W. W., Jr.: A Users Manual for ANISN, a One-Dimensional Discrete Ordinates Transport Code with Anisotropic Scattering, Computing Technology Center, Union Carbide Corporation, Document K-1693, 1967.
3. ZERBY, C. D.; and KELLER, F. S.: Nucl. Sci. Eng., vol. 27, 1967, p. 190.
4. SPENCER, L. V.: Phys. Rev., vol. 98, 1955, p. 1507.
5. McCORMICK, P. T.; KEIFFER, D. G.; and PARZEN, G.: Phys. Rev., vol. 103, 1956, p. 29.
6. MOLLER, C.: Ann. Physik, vol. 14, 1932, p. 531.
7. ROHRLICH, F.; and CARLSON, B. C.: Phys. Rev., vol. 93, 1954, p. 38.
8. BERGER, M. J.; and SELTZER, S. M.: Tables of Energy Losses and Ranges of Electrons and Positrons, NASA Document NASA-SP-3012, 1964.
9. STERNHEIMER, R. M.: Phys. Rev., vol. 103, 1956, p. 511.
10. GOUDSMIT, S. A.; and SAUNDERSON, J. L.: Phys. Rev., vol. 57, 1940, p. 24; and Phys. Rev., vol. 58, 1940, p. 36.
11. BERGER, M. J.: Monte Carlo Calculation of the Penetration and Diffusion of Fast Charged Particles, p. 149 in Methods in Computational Physics, Vol. I, eds. B. Adler, S. Fernbach, and M. Rotenberg, Academic Press, New York, 1963.
12. RESTER, D. H.; and RAINWATER, W. J.: Investigations of Electron Interactions with Matter, NASA Document CR-334, 1965.
13. RESTER, D. H.; and DANCE, W. E.: Investigation of Electron Interaction with Matter, LTV Report No. 0-71000/6R-18, 1966.
14. SCOTT, W. W.: Comparisons of the Results Obtained with Several Electron-Penetration Codes, Oak Ridge National Laboratory Document ORNL RSIC-28, 1970.
15. CARTER, R. E., et al.: Phys. Rev., vol. 113, 1959, p. 280.